Capabilities of a novel electrochemical cell for *operando* XAS and SAXS investigations for PEM fuel cells and water electrolysers

Marco Bogar[1], Yurii Yakovlev[2], Simone Pollastri[3,4], Roberto Biagi[3,5,6], Heinz Amenitsch[7], Rodolfo Taccani[1], Iva Matolínová[2]

[1] Department of Engineering and Architecture, University of Trieste, Via Alfonso Valerio 6/1, 34127 Trieste, Italy

[2] Department of Surface and Plasma Science, Faculty of Mathematics and Physics, Charles University, V Holešovičkách 2, 180 00 Prague 8, Czech Republic.

[3] Department of Physics, Computer Science and Mathematics, University of Modena and Reggio Emilia, 41125, Modena, Italy

[4] ELETTRA - Sincrotrone Trieste S.C.p.A., SS 14 - km 163,5, 34149, Basovizza, Trieste, Italy.

[5] Istituto Nanoscienze (NANO-S3), Consiglio Nazionale delle Ricerche (CNR), via G. Campi 213/a, Modena, 41125, Italy

[6] Centro H2-MORE, Univeristy of Modena and Reggio Emilia, 41125, Modena, Italy

[7] Graz University of Technology, Institute for Inorganic Chemistry, Stremayrgasse 9, 8010 Graz, Austria.

Supplementary Materials

Data citation

To promote open access policies and data reproducibility, the raw files of the data shown in this paper are available at the following DOI: 10.5281/zenodo.10907414.

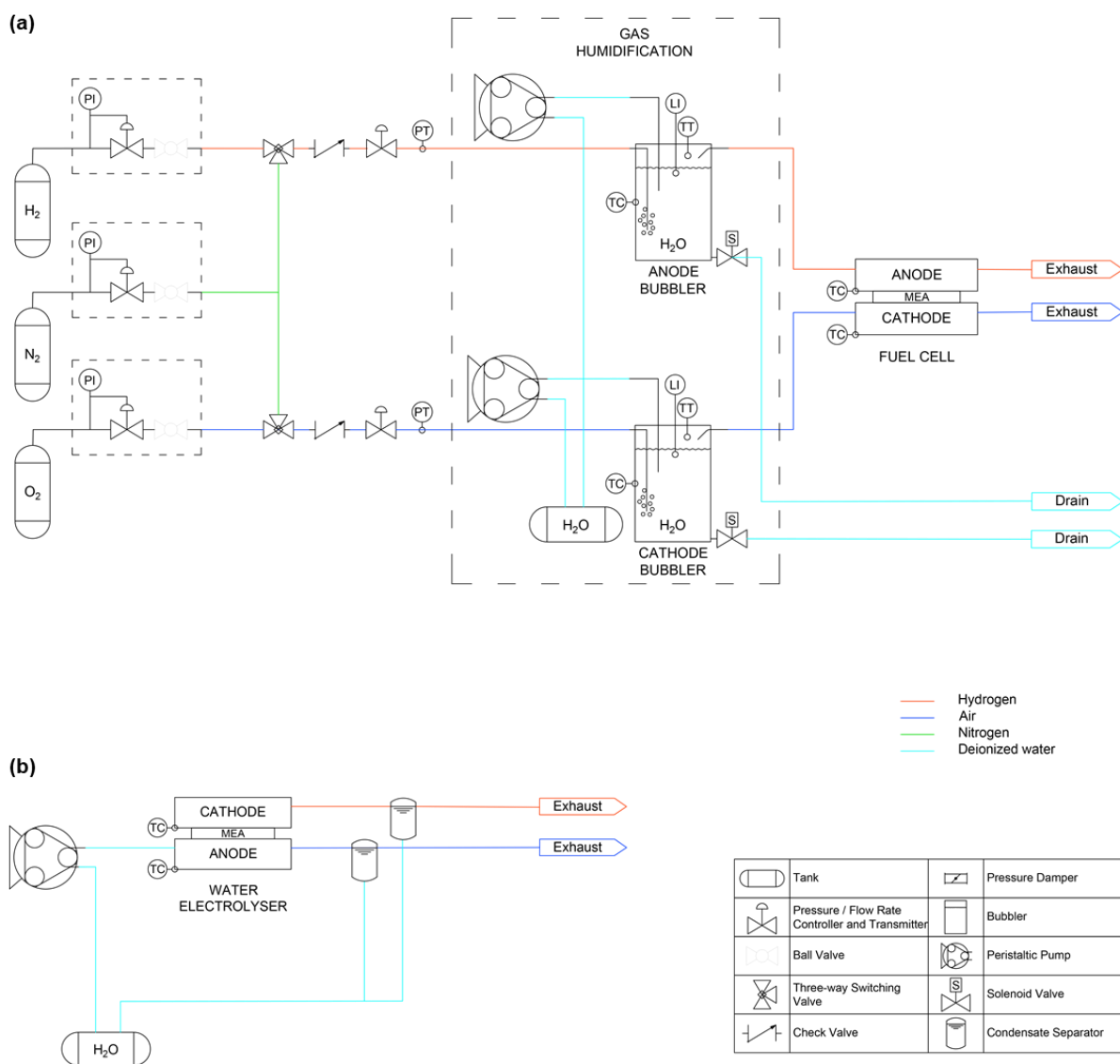### Supplementary Figures

Figure S1. P&ID of the electrochemical cell and the control station with the cell operating (a) as a PEMFC and (b) as a PEMWE.
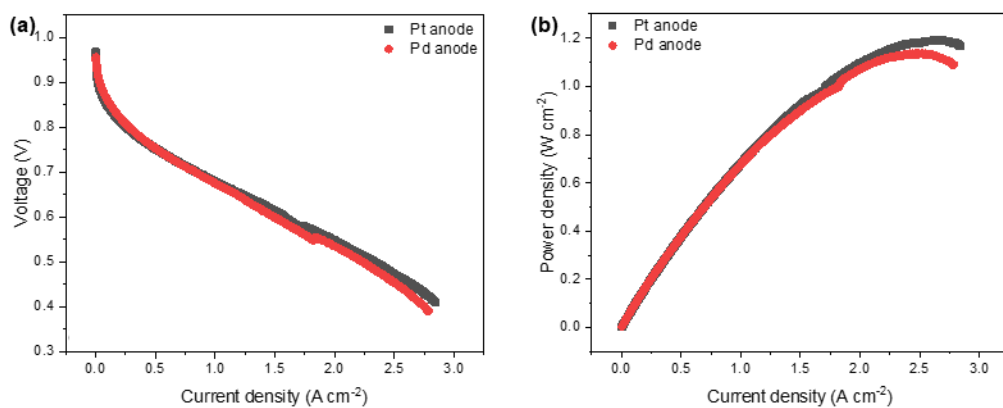
Figure S2. Pt and Pd as catalysts for FC anode electrode. Comparison of voltage-current (a) and power-current (b) response of Pt and Pd based anodes. Commercial GDEs with catalyst loading of $0.3mg_{Pt}$ cm^{-2} were used as a cathode.
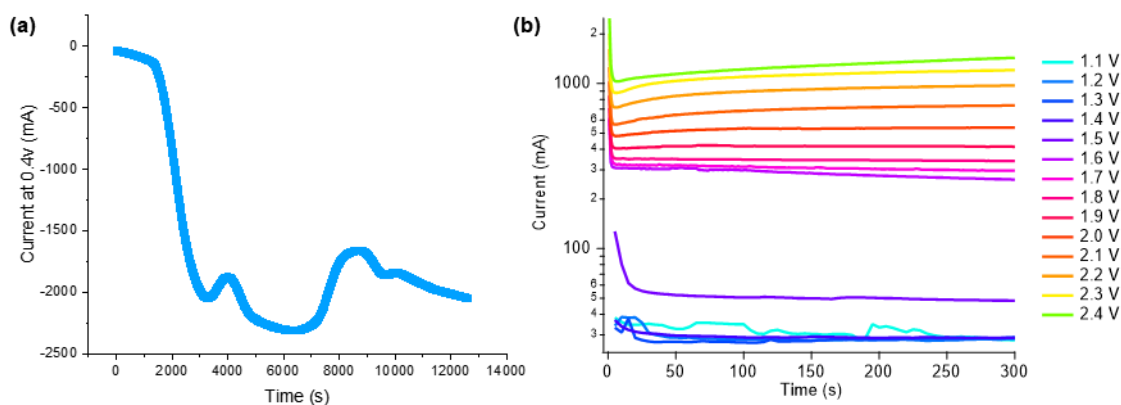

Figure S3. Break-in procedures. (a) In fuel cell mode, performance of Pt/Carbon catalyst during break-in process where current was measured as a function of time at constant voltage of 0.4 V. (b) In water electrolysis mode, potentiostatic curves recorded during water electrolyzer operation at different cell voltages.
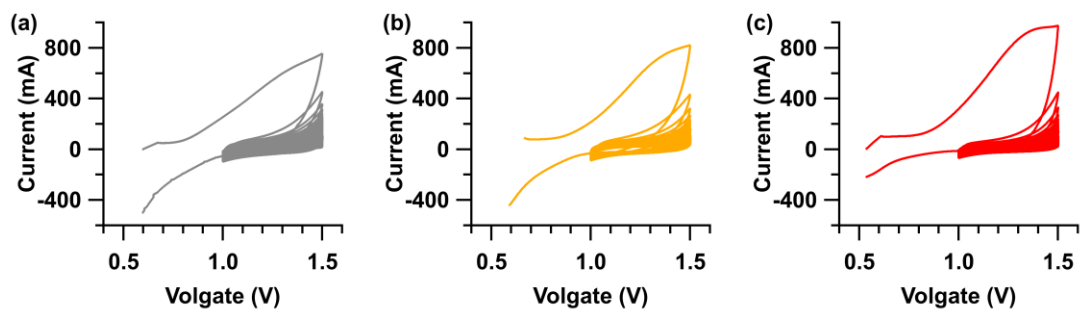
Figure S4. Accelerated stress tests. Evolution of cyclic voltammograms constituting AST, run from 1.0 to 1.5 V at the sweep rate of 500 mV·s^{-1}, and recorded within: (a) 0 ÷ 500, (b) 500 ÷ 1000, and (c) 1000 ÷ 2000 cycles.
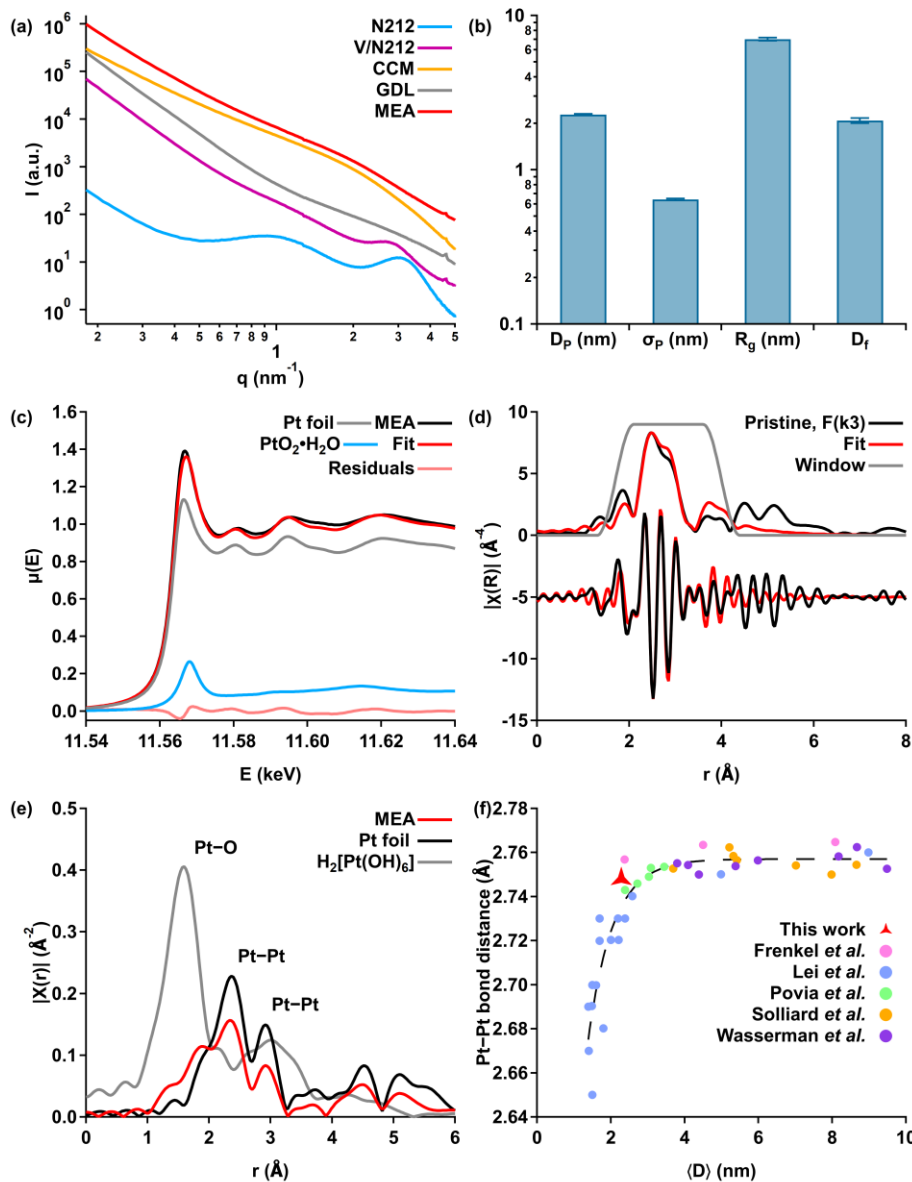
Figure S5. MEA characterization in pristine conditions. (a) Vertically shifted scattering pattern of the whole MEA and of the layers composing it: bare Nafion (N212), Vulcan deposited onto Nafion (V/N212), Catalyst Coated Membrane (CCM), Gas Diffusion Layer (GDL), complete MEA. The scattering pattern of the single components were obtained via *ex situ* measurements. The scattering patter of the MEA was recorded at the beginning of *in operando* measurements, before running the conditioning protocol. (b) main results from fitting the scattering patter of the MEA in pristine conditions with the analytical model: mean particle diameter (D_P) and standard deviation (σ_P) within the Schulz distribution, average cluster size represented by the Radius of gyration (R_g) calculated from the cut-off length (ξ), and fractal dimension (D_f). XAS analyses of the MEA in pristine conditions,

measured *ex situ* at the Pt L$_3$-edge: (c) LCF of the XANES spectrum; (d) first shell EXAFS refinement: the k3 Fourier transform of the pristine trace (Pristine, F(k3), black line), the obtained fit (red line) and the used window (grey line) supplied with the real part (lower graphs); (e) Fourier transformed EXAFS spectrum of the MEA compared with the spectra from a Pt metal foil and H$_2$[Pt(OH)$_6$]reference compound (from XAFS beamline database). (f) Pt–Pt bond distance (retrieved from EXAFS analysis) is plotted against the mean particle diameter (obtained from SAXS analysis). The obtained result is compared with the values reported in literature by Frankel *et al.*[1], Lei *et al.*[2], Povia *et al.*[3], Solliard *et al.*[4], and Wasserman *et al.*[5].
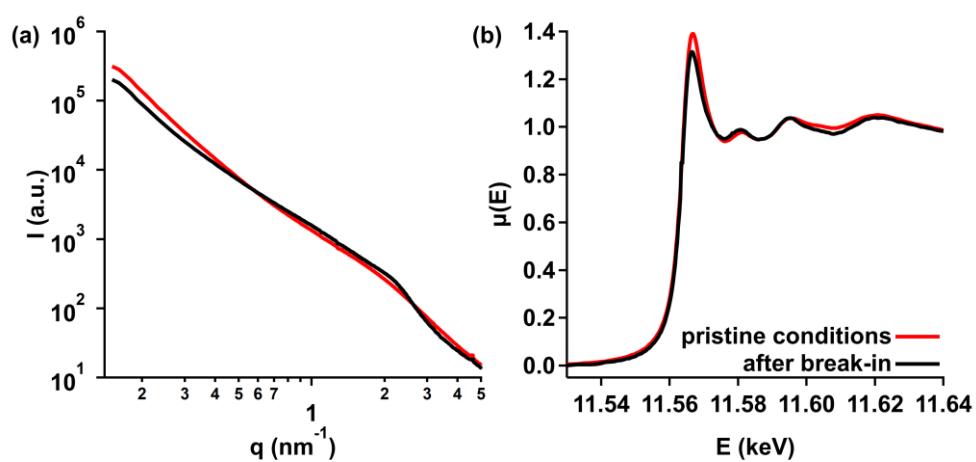

Figure S6. The break-in procedure. Comparison of (a) the SAXS patterns and (b) the XAS spectra recorded from the MEA in pristine conditions (red) and after the (conditioning and) break-in procedure (black).
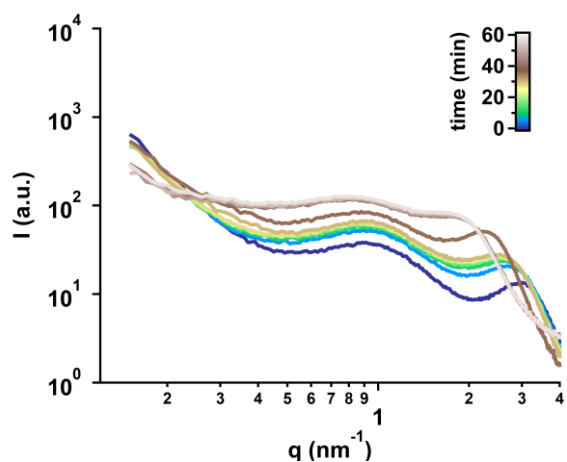
Figure S7. The effects of the conditioning protocol on the MEA components. Time resolved scattering patterns recording *in situ* the evolution of (a) Nafion during the conditioning protocol.
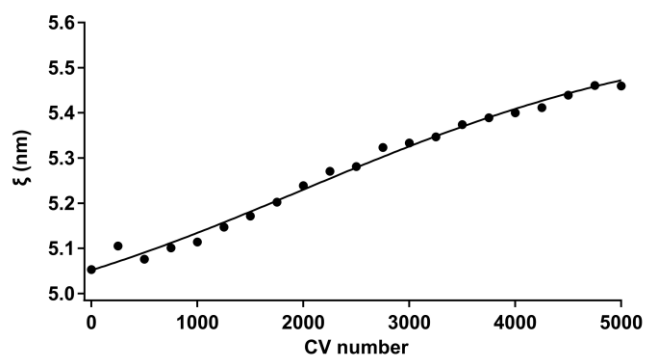

Figure S8. Scattering correlation length. Evolution of scattering correlation length calculated over the scattering patters represented in Figure 3b within the range: $0.20 \div 1.80$ nm^{-1}. The fill line is a guideline for the sight only.
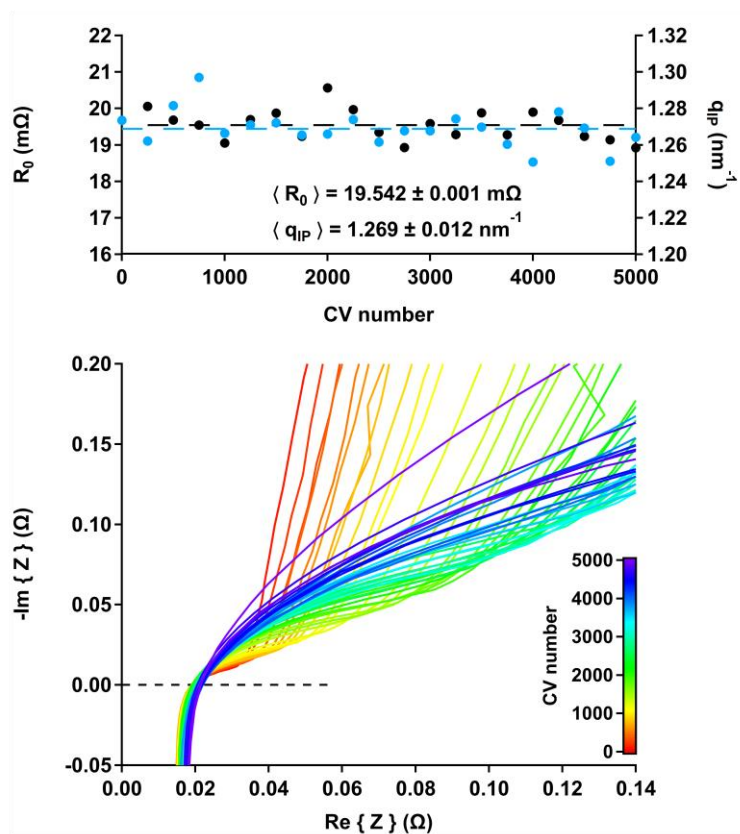
Figure S9. PEIS and SAXS. Time resolved PEIS during AST is show in the main graph, on the bottom. On top, the corresponding value of the membrane resistance (R_0) is compared with respect to the position of the ionomer peak (q_{IP}), retrieved from fitting with the analytical model the SAXS patterns shown in Figure 2b.
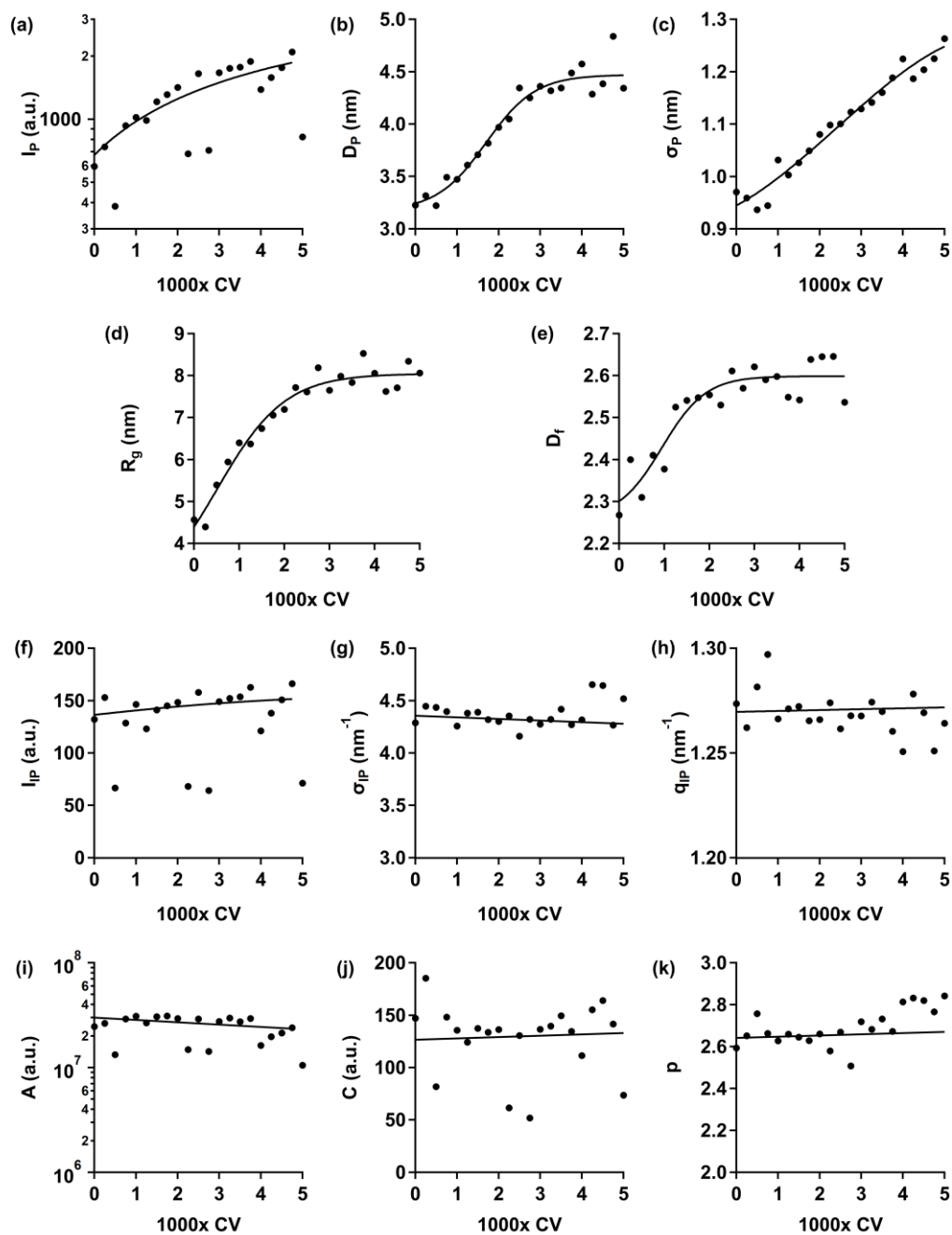
Figure S10. SAXS fitting: complete results. Time resolved evolution of the parameters composing the analytical model used for fitting the SAXS patterns represented in Figure 2. Parameters modelling the catalyst nanoparticles are show in the first two lines; form factor parameters: (a) forwarded scattering probability, (b) mean particle size, and (c) standard deviation within the size distribution. Structure factor parameters: (d) radius of gyration (calculated from the cut-off length, ξ), and (e) fractal dimension. Parameters modelling the ionomer peak from Nafion substrate: Voigt peak: (f) intensity, (i) width, and (h) position; the shape parameter was kept constant to 0.45, value retrieved from fitting the

bare Nafion membranes (Figure S7), as done in a previous work[6]. Parameters modelling the Vulcan substrate: (i) forwarded scattering probability from the Debye-Anderson-Brumberger model, where the correlation length was kept fixed to 36.07 nm, as previously done[6]. Parameters modelling the GDL: (j) forwarded scattering probability, and (k) exponent of the power law term. Fill lines are a guide for the sight only.
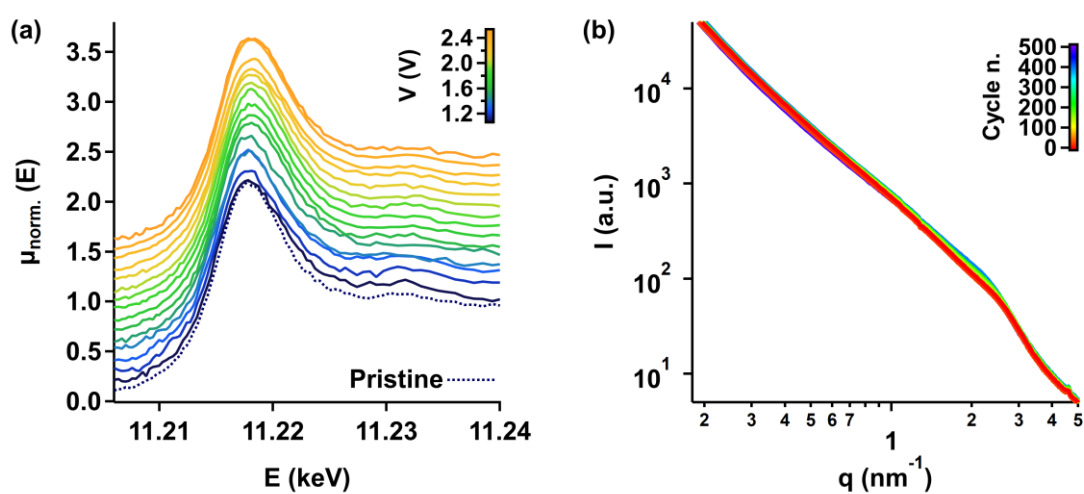

Figure S11. *In operando* **water electrolysis.** (a) The normalized XANES spectra collected *in operando* at the Ir L_3-edge recorded while running AST, are compared with the spectrum recorded *ex situ* in pristine conditions. (b) Time-resolved *in operando* SAXS patterns recorded while running AST.

References

[1]   A. I. Frenkel, C. W. Hills, and R. G. Nuzzo, "A view from the inside: Complexity in the atomic scale ordering of supported metal nanoparticles," *J. Phys. Chem. B*, vol. 105, no. 51, pp. 12689–12703, Dec. 2001, doi: 10.1021/jp012769j.

[2]   Y. Lei, J. Jelic, L. C. Nitsche, R. Meyer, and J. Miller, "Effect of particle size and adsorbates on the L3, L2 and L1 X-ray absorption near edge structure of supported Pt nanoparticles," *Top. Catal.*, vol. 54, no. 5–7, pp. 334–348, 2011, doi: 10.1007/s11244-011-9662-5.

[3]   M. Povia *et al.*, "Combining SAXS and XAS to Study the Operando Degradation of Carbon-Supported Pt-Nanoparticle Fuel Cell Catalysts," *ACS Catal.*, vol. 8, no. 8, pp. 7000–7015, 2018, doi: 10.1021/acscatal.8b01321.

[4]   C. Solliard and M. Flueli, "Surface stress and size effect on the lattice parameter in small particles of gold and platinum," *Surf. Sci.*, vol. 156, no. PART 1, pp. 487–494, 1985, doi: 10.1016/0039-6028(85)90610-7.

[5]   H. J. Wasserman and J. S. Vermaak, "On the determination of the surface stress of copper and platinum," *Surf. Sci.*, vol. 32, no. 1, pp. 168–174, 1972, doi: 10.1016/0039-6028(72)90127-6.

[6]   M. Bogar *et al.*, "A small angle X-ray scattering approach for investigating fuel cell catalyst degradation for both ex situ and in operando analyses," *Int. J. Hydrogen Energy*, vol. 58, no. January, pp. 1673–1681, Mar. 2024, doi: 10.1016/j.ijhydene.2024.01.261.